Research Article
Open Access

MJ Engineering Sciences

Available at: https://mjcellpress.com/article/mjes15/

Nonlinear Analysis And Control Of The Dynamic Behaviour of A Pipeline Conveying Fluid With Time-Dependent Velocity

Barthelemy Roger Lekoa [1,*], Lionel Merveil Anague Tabejieu[1,2], Marina Aude Nguessom Foadieng [1], Nelson Kevin Foadieng Fokam[3], Valéry Claude Abbe Ngayihi [1]

[1]Laboratory of Mechanics and Materials, Department of Mechanical Engineering, National Higher Polytechnic School of Douala, University of Douala, P.O Box 2701, Douala, Cameroon.
[2]Laboratory of Modelling and Simulation in Engineering, Biomimetics and Prototypes and TWAS research unit, Faculty of Science, University of Yaoundé I, P.O. 812, Yaoundé, Cameroon.
[3]Laboratory of Mechanics and Materials, Department of Civil Engineering, National Higher Polytechnic School of Douala, University of Douala, P.O Box 2701, Douala, Cameroon

[*]Corresponding authors: rogerlekoa@gmail.com

Key words

Pipeline conveying fluid, Time-dependent velocity, Nonlinear vibration; Critical mean flow velocity, Nonlinear energy sink, Vibration control.

Abstract

Pipelines conveying pulsating fluids are prone to complex vibration phenomena that may compromise their structural stability and reduce their service life. This study investigates the nonlinear dynamic behavior of a simply supported pipeline conveying a fluid with time-dependent velocity. Both the uncontrolled configuration and the configuration equipped with a vibration controller are considered. The governing equations are derived using the generalized Hamiltonian variational principle, Euler–Bernoulli beam theory, and von Kármán nonlinear strain–displacement relations. The critical mean flow velocities associated with the first and second vibration modes are determined, and their influence on the temporal displacement response of the pipeline is analyzed. A nonlinear energy sink is then introduced as a passive vibration control device to reduce the transverse vibration amplitude of the system. The results show that, for mean flow velocities below the critical value, the pipeline vibrates around a stable equilibrium point, whereas velocities equal to or greater than the critical value led to vibrations around an unstable equilibrium point. The proposed vibration controller reduces the vibration amplitude by 51%, thereby improving the dynamic stability of the pipeline. However, a dedicated stability analysis remains necessary to identify optimal controller parameters for enhanced vibration attenuation.

Received:26.01.2026 Accepted: 02.05.2026 Published online: 09.07.2026

How to cite this article: Lekoa, B. R., Anague Tabejieu, L. M., Nguessom Foadieng, M. A., Foadieng Fokam, N. K., & Abbe Ngayihi, V. C. (2026). *Nonlinear analysis and control of the dynamic behaviour of a pipeline conveying fluid with time-dependent velocity*. *MJ Engineering Sciences*. *MJ Engineering Sciences*. MJ Engineering Sciences. *2*(2), 216-240. https://doi.org/10.63156/mjes15

1. Introduction

The transportation of fluids through flexible pipelines is fundamental to numerous engineering applications, including submarine oil and gas transportation systems, hydropower facilities, and biological engineering devices (Tang et al., 2022a). During operation, these structures are subjected to complex dynamic loads that can induce significant vibration phenomena (Hao et al., 2023a). Among the various excitation mechanisms, vibrations generated by pulsating fluid flow are particularly prevalent and are recognized as one of the most critical sources of structural instability in engineering systems (Wei et al., 2023a). Such vibrations considerably influence the natural frequencies, dynamic stability, and fatigue life of pipelines, potentially leading to structural failure and substantial economic losses (Gao et al., 2021; Hao et al., 2023a). Consequently, understanding the dynamic behavior of fluid-conveying pipelines and developing effective vibration mitigation strategies remain important challenges in structural dynamics.

Over the past decades, the dynamic response of pipelines conveying pulsating fluids has attracted considerable research interest. Panda and Kar (2007) investigated the nonlinear dynamics of fluid-conveying pipes with particular emphasis on parametric and internal resonances. Hao et al. (2023a) analyzed the stability and nonlinear response of elastically constrained pipes subjected to parametric excitation induced by pulsating flow. Wei et al. (2023a) examined the parametric vibration characteristics of nonlinearly supported pipes conveying pulsating fluids, whereas Tan and Ding (2020) investigated the parametric resonances of Timoshenko pipes conveying high-speed pulsating fluids. Yang et al. (2014) proposed passive and adaptive vibration suppression strategies for pipes conveying fluids with variable velocity. Mao et al. (2016) studied the steady-state response of a fluid-conveying pipe exhibiting a 3:1 internal resonance in the supercritical regime. Kesimli et al. (2016) investigated the free vibration characteristics of fluid-conveying pipes with intermediate supports. Tang et al. (2022b) examined the nonlinear fractional-order dynamic stability of viscoelastic fluid-conveying pipes subjected to time-dependent flow velocity. Luo and Zhang (2022) analyzed the dynamic behavior of an axially moving underwater pipe conveying pulsating fluid. Karrech et al. (2024) investigated the nonlinear vibration of free-spanning subsea pipelines by accounting for multidimensional mid-plane stretching. Cao et al. (2025) explored vibration mitigation and the dynamic response of pipeline systems equipped with a nonlinear soft clamp employing a nonlinear energy sink (NES). Zhou et al. (2021) analyzed the nonlinear dynamics of L-shaped fluid-conveying pipes using the absolute nodal coordinate formulation, while Wang et al. (2022) investigated the vibration behavior of marine risers during shallow- and deep-water installation processes.

Although these studies have significantly advanced the understanding of the dynamics of fluid-conveying pipelines, they have primarily focused on parametric resonance, nonlinear response, and stability analyses. In parallel, numerous investigations have demonstrated, through both theoretical and experimental approaches, that linear and nonlinear vibration control techniques can effectively enhance structural stability by substantially reducing vibration amplitudes (Mamaghani et al., 2016; Yang et al., 2019; Zhang et al., 2023; Zhao et al., 2018a). However, the vibration control of pipelines conveying fluids with time-dependent velocity has received comparatively limited attention and therefore remains an important research topic.

In the present study, the nonlinear dynamic behavior of a pipeline conveying a fluid with time-dependent velocity is investigated. Particular emphasis is placed on evaluating the influence of the critical mean flow velocity on the natural frequencies and dynamic response of the pipeline. To reduce the resulting vibrations, a nonlinear energy sink (NES) is introduced as a passive vibration control device, and its effectiveness is assessed through a comparative analysis of the uncontrolled and controlled systems. The results provide further insight into the dynamic behavior of fluid-conveying pipelines operating under time-dependent flow conditions and demonstrate the capability of the proposed NES to improve both vibration attenuation and the overall dynamic stability of the system.

2. Model Description

The physical system considered in this study consists of a uniform pipeline conveying an internal fluid with a time-dependent velocity. As illustrated in Figure 1(a), the pipeline is simply supported at both ends and is subjected to a harmonic fluctuation of the internal flow velocity. The corresponding equivalent lumped-parameter model is shown in Figure 1(b). The pipeline has a length L, where x denotes the spatial coordinate measured along the neutral axis and t represents time. The fluid and pipeline densities are denoted by ρ_f and ρ_p, respectively, while A_f and A_p represent the cross-sectional areas of the fluid and the pipeline.

The internal flow velocity is assumed to fluctuate harmonically about a constant mean value (Hao et al., 2023b; Tang et al., 2022b; Wei et al., 2023b), according to $V = V_0 + V_1 \cos(\Omega t)$, where V_0 is the average and constant fluid velocity, V_1 and Ω are the amplitude and frequency of the fluctuation, respectively. In order to derive the equations of motion, the following assumptions are made: (i) the deformation of the pipeline conveying fluid is limited in a plane; (ii) the Euler-Bernoulli beam theory with geometric nonlinearities is adopted (in order to take into account the large deformations), and the influences of rotary inertia and shearing deformation are neglected; (iii) variations of cross sectional dimensions are negligible; (iv) the pipeline system is subjected to no external loads; $w(x,t)$ and $u(x,t)$, represent the transverse and longitudinal displacements, respectively, which can specify the coupled planar motion of the pipeline.

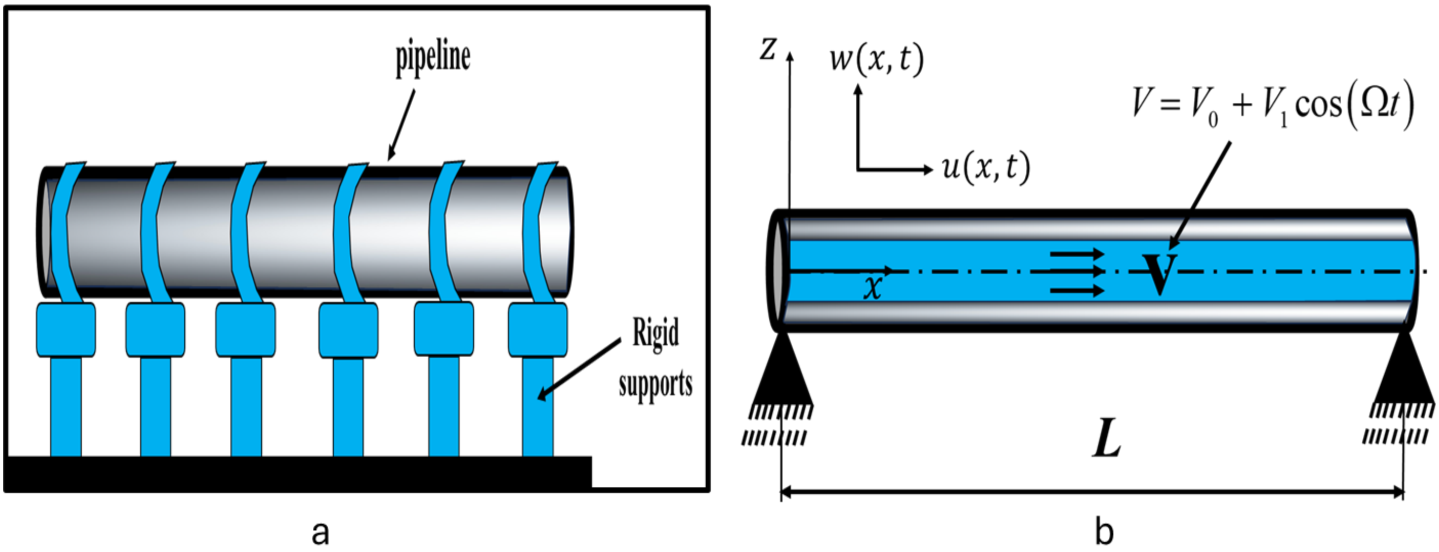

Figure 1: Physical model of the pipeline conveying fluid: (a) physical configuration and (b) equivalent lumped-parameter model.

2.1. Formulation of the Mathematical Model

The mathematical model governing the coupled planar motion of the pipeline conveying a fluid with time-dependent velocity is established using the generalized Hamiltonian variational principle (Dai et al., 2015a; Wang, Hu, & Zhong, 2013a), which is expressed as follows:

$$\int_{t_1}^{t_2} \delta(T-U)\, dt + \int_{t_1}^{t_2} \delta W_{nc}\, dt = 0 \tag{1}$$

where T, U, W_{nc} denote the total kinetic energy, the total potential energy, and the virtual work performed by the internal non-conservative and external forces acting on the pipeline system, respectively.

The total kinetic energy of the system is obtained by summing the kinetic energy of the conveyed fluid, T_f, and that of the pipeline structure, T_p, such that

$$T = T_p + T_f \tag{2}$$

According to assumptions (i) and (ii) introduced in the previous section, the kinetic energies T_f and T_p can be expressed as follows (Dai et al., 2015a; Wang et al., 2013a):

$$\begin{cases} T_p = \dfrac{1}{2}\rho_p A_p \displaystyle\int_0^L \left[\left(\dfrac{\partial u}{\partial t}\right)^2 + \left(\dfrac{\partial w}{\partial t}\right)^2\right] dx \\ T_f = \dfrac{1}{2}\rho_f A_f \displaystyle\int_0^L \left[\left(V + \dfrac{\partial u}{\partial t} + V\dfrac{\partial u}{\partial x}\right)^2 + \left(\dfrac{\partial w}{\partial t} + V\dfrac{\partial w}{\partial x}\right)^2\right] dx \end{cases} \tag{3}$$

Similarly, the total potential energy is defined as the sum of the strain energy associated with the stress variation from the initial configuration of the pipeline, U_p, and the strain energy resulting from the subsequent axial stretching, U_t, namely

$$U = U_p + U_t \tag{4}$$

Based on assumptions (i) and (iii), the expressions of U_p and U_t are given by (Dai et al., 2015a; Wang et al., 2013a):

$$\begin{cases} U_p = \dfrac{1}{2}\displaystyle\int_0^L \int_{A_p} E\left(-z\dfrac{\partial^2 w}{\partial x^2} + \sqrt{\left(1+\dfrac{\partial u}{\partial x}\right)^2 + \left(\dfrac{\partial w}{\partial x}\right)^2} - 1\right)^2 dA dx \\ U_t = \displaystyle\int_0^L \left[P\sqrt{\left(1+\dfrac{\partial u}{\partial x}\right)^2 + \left(\dfrac{\partial w}{\partial x}\right)^2} - 1\right] dx \end{cases} \tag{5}$$

where z denotes the coordinate measured from the neutral plane of the pipeline cross-section, and P represents the axial pressure induced by the internal fluid flow.

According to assumption (iv), the virtual work associated with the internal non-conservative forces and the external forces can be written as

$$\int_{t_1}^{t_2}\int_0^L \delta W_{nc}\, dx\, dt = \int_{t_1}^{t_2}\int_0^L \left(-c\frac{\partial w}{\partial t}\right)\delta w\, dx\, dt \tag{6}$$

where c denotes the viscous damping coefficient of the pipeline.

Substituting Eqs. (2)–(7) into Eq. (1) and applying the integration-by-parts procedure yields the governing equations of motion

$$\begin{cases} \left(\rho_p A_p + \rho_f A_f\right)\dfrac{\partial^2 u}{\partial t^2} + 2\rho_f A_f\left(V_0 + V_1\sin(\Omega t)\right)\dfrac{\partial^2 u}{\partial x \partial t} + \rho_f A_f\left(V_0 + V_1\sin(\Omega t)\right)^2\dfrac{\partial^2 u}{\partial x^2} \\ \qquad + \rho_f A_f \dfrac{dV}{dt}\dfrac{\partial u}{\partial x} - \dfrac{\partial}{\partial x}\left(\dfrac{\left(\sigma_N A_p + P\right)\left(1+\dfrac{\partial u}{\partial x}\right)}{\sqrt{\left(1+\dfrac{\partial u}{\partial x}\right)^2 + \left(\dfrac{\partial w}{\partial x}\right)^2}}\right) = 0 & \text{(7a)} \\ \left(\rho_p A_p + \rho_f A_f\right)\dfrac{\partial^2 w}{\partial t^2} + 2\rho_f A_f\left(V_0 + V_1\sin(\Omega t)\right)\dfrac{\partial^2 w}{\partial x \partial t} + \rho_f A_f\left(V_0 + V_1\sin(\Omega t)\right)^2\dfrac{\partial^2 w}{\partial x^2} \\ \qquad + \rho_f A_f \dfrac{dV}{dt}\dfrac{\partial w}{\partial x} + c\dfrac{\partial w}{\partial t} + EI\dfrac{\partial^4 w}{\partial x^4} - \left(\dfrac{\left(\sigma_N A_p + P\right)\left(\dfrac{\partial^2 w}{\partial x^2}\right)}{\sqrt{\left(1+\dfrac{\partial u}{\partial x}\right)^2 + \left(\dfrac{\partial w}{\partial x}\right)^2}}\right) = 0 & \text{(7b)} \end{cases}$$

where

$$V = V_0 + V_1 \cos(\Omega t) \quad \text{and} \quad \sigma_N = E\left(\sqrt{\left(1+\frac{\partial u}{\partial x}\right)^2 + \left(\frac{\partial w}{\partial x}\right)^2} - 1\right) \tag{8}$$

Since the nonlinear vibration considered in this study corresponds to a small but finite stretching problem, the coupling between the longitudinal and transverse motions is neglected, while only the lowest-order nonlinear terms are retained. Furthermore, both the longitudinal and transverse displacements are assumed to remain much smaller than the pipeline length. Consequently, u, w, and their spatial derivatives are treated as small quantities. Under these assumptions, the Taylor series expansion can be expressed as (Tang, Zhen, & Fang, 2018):

$$\left(\left(1+\frac{\partial u}{\partial x}\right)^2 + \left(\frac{\partial w}{\partial x}\right)^2\right)^{-\frac{1}{2}} \approx 1 - \frac{\partial u}{\partial x} - \frac{1}{2}\left(\frac{\partial w}{\partial x}\right)^2 \tag{9}$$

and

$$\sigma_N = E\left(\frac{\partial u}{\partial x} + \frac{1}{2}\left(\frac{\partial w}{\partial x}\right)^2\right) \tag{10}$$

Assuming that the initial axial tension P remains constant, substituting Eqs. (10) and (11) into Eqs. (7a) and (7b), while neglecting the effects of longitudinal inertia together with higher-order nonlinear terms, leads to:

$$\frac{\partial}{\partial x}\left[\frac{\partial u}{\partial x} + \frac{1}{2}\left(\frac{\partial w}{\partial x}\right)^2\right] = 0 \tag{11}$$

$$\begin{aligned} &\left(\rho_p A_p + \rho_f A_f\right)\frac{\partial^2 w}{\partial t^2} + 2\rho_f A_f\left(V_0 + V_1 \sin(\Omega t)\right)\frac{\partial^2 w}{\partial x \partial t} + \rho_f A_f\left(V_0 + V_1 \sin(\Omega t)\right)^2 \frac{\partial^2 w}{\partial x^2} \\ &+ c\frac{\partial w}{\partial t} - P\frac{\partial^2 w}{\partial x^2} + EI\frac{\partial^4 w}{\partial x^4} + \rho_f A_f \frac{dV}{dt}\frac{\partial w}{\partial x} - EA_p \frac{\partial}{\partial x}\left[\frac{\partial w}{\partial x}\left(\frac{\partial u}{\partial x} + \frac{1}{2}\left(\frac{\partial w}{\partial x}\right)^2\right)\right] = 0 \end{aligned} \tag{12}$$

By integrating Eq. (12) twice with respect to ***x***, and applying the boundary conditions $(u = 0 \text{ at } x = 0,\ x = L)$, the following expression is obtained:

$$u(x) = \frac{x}{2L}\int_0^L \left(\frac{\partial w}{\partial x}\right)^2 dx - \frac{1}{2}\int_0^x \left(\frac{\partial w}{\partial x}\right)^2 dx \tag{13}$$

Substituting Eq. (12) into Eq. (13) finally yields

$$\begin{aligned} &\left(\rho_p A_p + \rho_f A_f\right)\frac{\partial^2 w}{\partial t^2} + 2\rho_f A_f\left(V_0 + V_1 \sin(\Omega t)\right)\frac{\partial^2 w}{\partial x \partial t} + \rho_f A_f\left(V_0 + V_1 \sin(\Omega t)\right)^2 \frac{\partial^2 w}{\partial x^2} \\ &+ c\frac{\partial w}{\partial t} - P\frac{\partial^2 w}{\partial x^2} + EI\frac{\partial^4 w}{\partial x^4} + \rho_f A_f \frac{dV}{dt}\frac{\partial w}{\partial x} - \frac{EA_p}{2L}\frac{\partial^2 w}{\partial x^2}\int_0^L \left(\frac{\partial w}{\partial x}\right)^2 dx = 0 \end{aligned} \tag{14}$$

Equation (14) constitutes the nonlinear governing equation describing the transverse dynamic response of the pipeline conveying a fluid with time-dependent velocity.

For convenience, the following dimensionless variables are introduced:

$$x = L\xi;\ w = L\eta;\ \tau = \omega_0 t;\ \omega_0 = \frac{1}{L^2}\sqrt{\frac{EI}{M}};\ \Psi = \frac{\Omega}{\omega_0};\ \mu = \frac{cL^2}{\sqrt{EIM}};\ \beta = \frac{\rho_f A_f}{\rho_p A_p + \rho_f A_f}$$
$$\vartheta_0 = V_0 L\sqrt{\frac{\rho_f A_f}{EI}};\ \vartheta_1 = V_1 L\sqrt{\frac{\rho_f A_f}{EI}};\ \gamma = \frac{PL^2}{EI};\ \kappa = \frac{A_p L^2}{2I};\ M = \rho_p A_p + \rho_f A_f \tag{15}$$

Substituting these variables into Eq. (14) leads to the following dimensionless governing equation:

$$\frac{\partial^2\eta}{\partial\tau^2} + \frac{\partial^4\eta}{\partial\xi^4} + \mu\frac{\partial\eta}{\partial\tau} + 2\sqrt{\beta}\vartheta_0\frac{\partial^2\eta}{\partial\tau\partial\xi} + \left(\vartheta_0^{\,2} - \gamma\right)\frac{\partial^2\eta}{\partial\xi^2} - \kappa\frac{\partial^2\eta}{\partial\xi^2}\int_0^1\left(\frac{\partial\eta}{\partial\xi}\right)^2 d\xi =$$
$$-2\sqrt{\beta}\vartheta_1\sin\left(\Psi\tau\right)\frac{\partial^2\eta}{\partial\tau\partial\xi} - 2\vartheta_0\vartheta_1\sin\left(\Psi\tau\right)\frac{\partial^2\eta}{\partial\xi^2} - \sqrt{\beta}\vartheta_1\Psi\cos\left(\Psi\tau\right)\frac{\partial\eta}{\partial\xi} \tag{16}$$

To facilitate the analytical treatment, the Galerkin assumed-mode approach is employed. Accordingly, the transverse displacement is approximated by the finite modal expansion

$$\eta\left(\xi,\tau\right) = \sum_{n=1}^{\infty} q_n\left(\tau\right)\sin\left(n\pi\xi\right) \tag{17}$$

where $q_n\left(\tau\right)$ denotes the generalized coordinate associated with the nth vibration mode, and $\varphi_n\left(\xi\right)$ represents the corresponding mode shape satisfying $\varphi_n\left(\xi\right) = \sin\left(n\pi\xi\right)$.

Substituting Eq. (17) into Eq. (16), multiplying the resulting equation by the corresponding mode shape, integrating over the pipeline length, and applying the orthogonality condition of the eigenfunctions lead to the following modal equation:

$$\ddot{q} + \mu\dot{q} + \left(\varpi^2 - \varsigma\sin\left(\Psi\tau\right)\right)q + \beta_1 q^3 = 0 \tag{18}$$

With: $\varsigma = 2\pi^2\vartheta_0\vartheta_1$; $\beta_1 = \dfrac{\pi^4\kappa}{2}$; $\varpi^2 = \pi^4 - \pi^2\left(\vartheta_0^2 - \gamma\right)$

3. Influence of the Mean Flow Velocity on the Vibration Frequency of the Pipeline

This section investigates the influence of the mean flow velocity of the internal fluid on the dynamic characteristics of the pipeline. In particular, the critical mean flow velocities corresponding to the first and second vibration modes are determined, and the associated bifurcation behaviour of the pipeline is analysed.

To this end, the governing equation of the transverse displacement is considered. By neglecting both the harmonic fluctuation of the flow velocity and the nonlinear term, the governing equation reduces to

$$\frac{\partial^2\eta}{\partial\tau^2} + \frac{\partial^4\eta}{\partial\xi^4} + \mu\frac{\partial\eta}{\partial\tau} + 2\sqrt{\beta}\vartheta_0\frac{\partial^2\eta}{\partial\tau\partial\xi} + \left(\vartheta_0^{\,2} - \gamma\right)\frac{\partial^2\eta}{\partial\xi^2} = 0 \tag{19}$$

Assuming that

$$\eta\left(\xi,\tau\right) = \varphi_n\left(\xi\right)e^{i\omega\tau} \tag{20}$$

Where φ_n represents natural vibration modes and ω represent complex pulsations. By substituting (20) in (19), we obtain:

$$\begin{cases} \vartheta_{0_{cr}} = \sqrt{(n\pi)^2 + \gamma} \\ f\left(\vartheta_{0_{cr}}\right) = \dfrac{1}{2\pi}\sqrt{(n\pi)^4 - (n\pi)^2\left(\vartheta_{0_{cr}}^2 - \gamma\right)} \end{cases} \tag{21}$$

Where $\vartheta_{0_{cr}}$ is the mean critical flow velocity of the internal fluid.

The geometrical and mechanical properties of the pipeline, together with the physical characteristics of the internal fluid adopted for the numerical simulations, are summarized in Table 1 (Wei et al., 2023b).

Table 1. Geometrical, mechanical, and fluid properties used in the numerical simulations.

Parameters/Units	Symbols	Values
External diameters (m)	D_{ex}	0.02
Internal diameters (m)	D_{in}	0.016
Length of the pipeline (m)	L	1
Young's Modulus (N/m^2)	E	$7,2\times10^{10}$
Moment of inertia (m^4)	I	$7,82\times10^{-7}$
Structural damping coefficient $(N.s/m^2)$	c	0.5
Density of fluid (kg/m^3)	ρ_f	1000
Velocity (m/s)	V_0	3
Pressure (N/m^2)	P	5×10^5
Density of pipeline (kg/m^3)	ρ_p	2700

Figure 3 illustrates the variation of the dimensionless natural frequency as a function of the dimensionless mean flow velocity. It can be observed that the dimensionless natural frequency varies with the increase in the mean flow velocity, leading to divergence in both the first and second vibration modes. The corresponding critical mean flow velocities are found to be 4.33 and 6.95, respectively.

Since the first vibration mode is dominant, the first divergence point defines the critical flow velocity of the system. Consequently, mean flow velocities lower than 4.33 correspond to the subcritical regime, in which the pipeline remains dynamically stable.

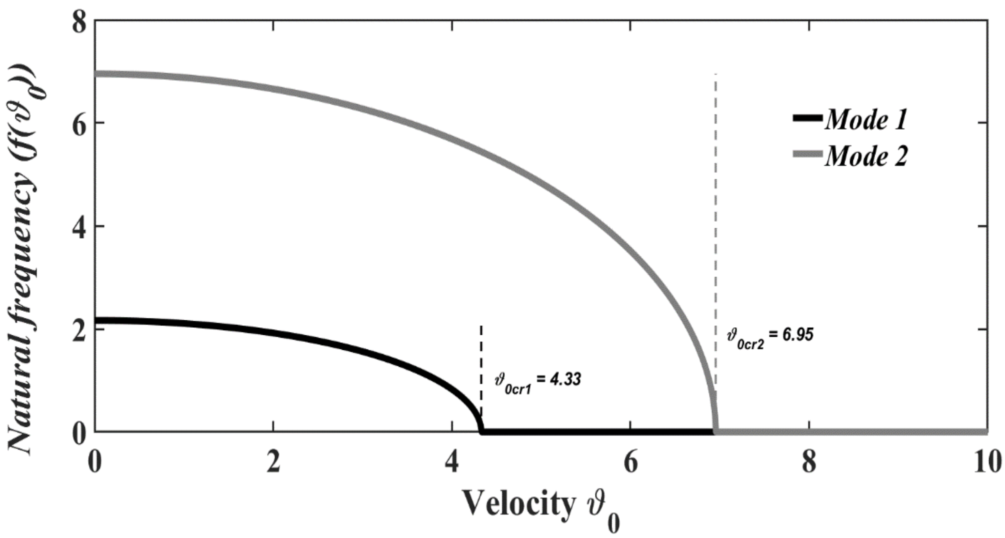

Figure 3. Evolution of the dimensionless natural frequency as a function of the dimensionless mean flow velocity

4. Influence of the Mean Flow Velocity on the Transverse Displacement Response of the Pipeline

This section examines the influence of the mean flow velocity on the transient transverse displacement response of the pipeline. The dimensionless time responses of the pipeline are obtained by numerically integrating the governing equation using the fourth-order Runge–Kutta method with a time step of $h = 0.01$ over the time interval $[0,100]$. The corresponding displacement histories are presented in Figures 4 and 5.

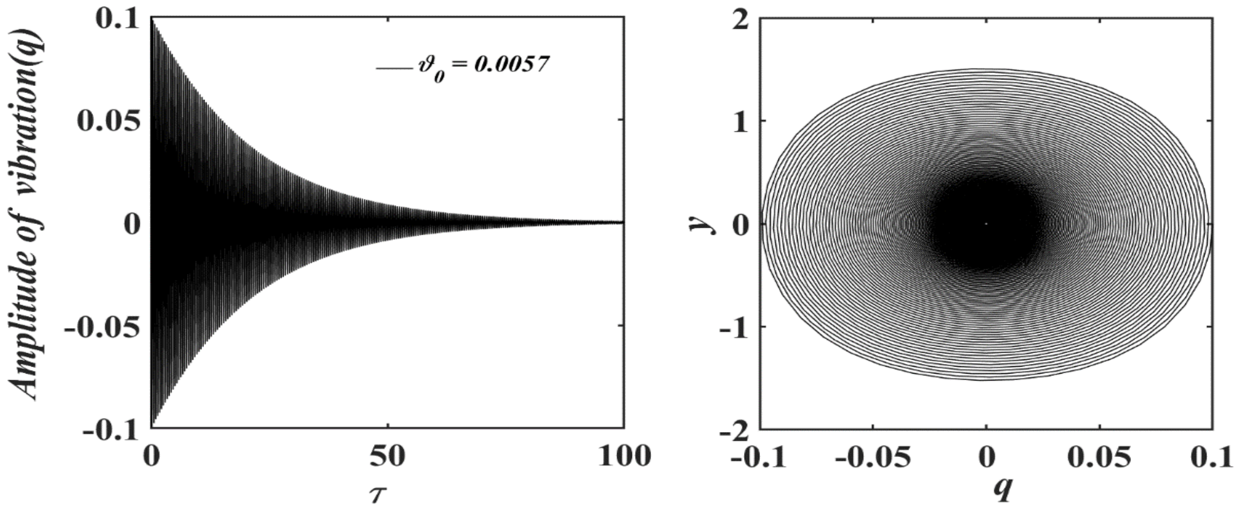

Figure 4: Time displacement response of the fluid conveying pipeline for a fluid velocity frequency of $\Omega = 13.60$ and $\vartheta_0 = 0.0057$.

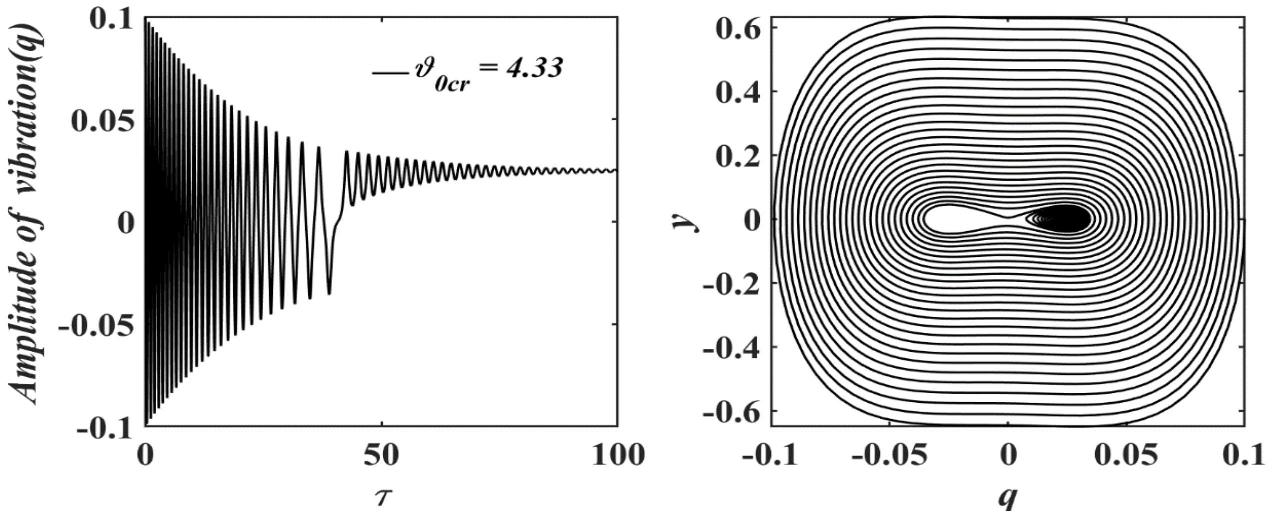

Figure 5: Time displacement response of the fluid conveying pipeline for a fluid critical velocity frequency of $\Omega = 13.60$ and $\vartheta_{0_{cr}} = 4.33$.

Figure 4 illustrates the time-history response of the pipeline conveying a fluid with time-dependent velocity for a flow excitation frequency of $\Omega = 13.60$ and a dimensionless mean flow velocity of $\vartheta_0 = 0.0057$. It can be observed that, when the dimensionless mean flow velocity remains below the critical value, the pipeline oscillates about a stable equilibrium position, indicating a dynamically stable operating regime.

In contrast, when the mean flow velocity reaches the critical value or exceeds it, the equilibrium state becomes unstable. This behaviour is illustrated in Figure 5, which presents the time response of the pipeline at the critical mean flow velocity $\vartheta_{0_{cr}} = 4.33$.. Under these conditions, the pipeline oscillates about an unstable equilibrium position, resulting in a significant deterioration of its dynamic stability. Such unstable oscillations may accelerate fatigue damage and considerably increase the risk of structural failure during long-term operation.

5. Suggestion of a Vibration Controller and Analysis of its Effects on The Dynamic Behaviour of the Pipeline

This section presents the dynamic response of the pipeline equipped with a vibration controller and evaluates its effectiveness in mitigating the vibrations induced by the fluctuating internal flow velocity. Particular attention is devoted to assessing the influence of the controller on the transverse displacement amplitude of the pipeline.
To this end, the same pipeline model described in the previous sections is considered, with the addition of a Nonlinear Energy Sink (NES) acting as a passive vibration absorber. The pipeline remains simply supported and is subjected to the same time-dependent internal flow velocity. The physical configuration of the controlled pipeline and the corresponding simplified model of the vibration controller are illustrated in Figures 6 and 7, respectively.

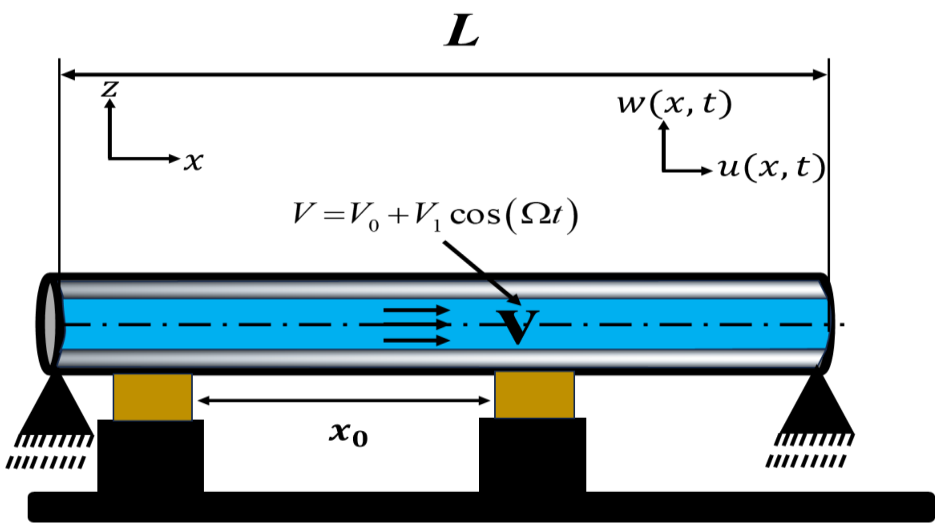

Figure 6. Physical model of the pipeline equipped with a vibration controller.

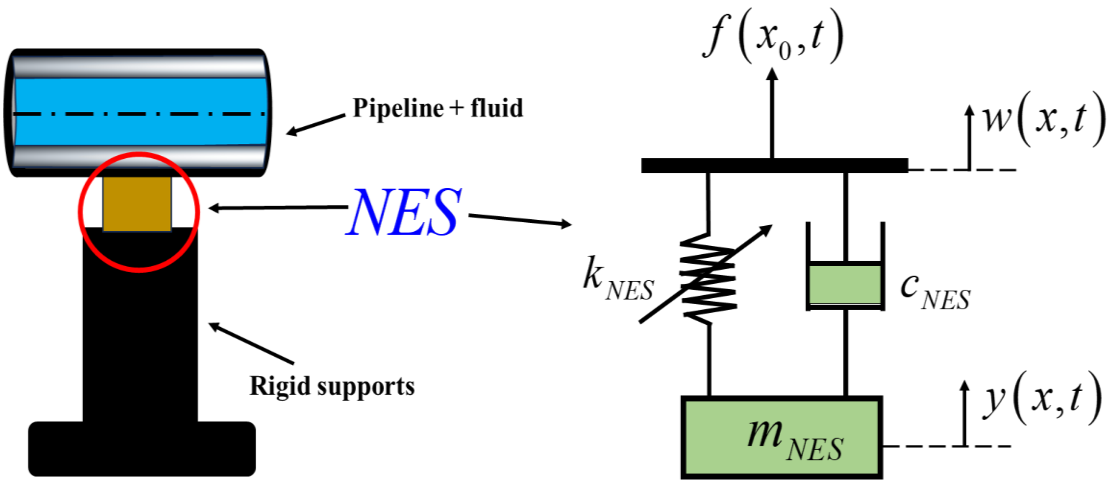

Figure 7. Simplified model of the vibration controller.

Using the same assumptions introduced previously, the equations governing the motion of the pipeline equipped with the vibration controller can be written as follows:

$$\begin{aligned}&\left(\rho_p A_p+\rho_f A_f\right)\frac{\partial^2 w}{\partial t^2}+2\rho_f A_f\left(V_0+V_1\sin(\Omega t)\right)\frac{\partial^2 w}{\partial x\partial t}+\rho_f A_f\left(V_0+V_1\sin(\Omega t)\right)^2\frac{\partial^2 w}{\partial x^2}\\&+c\frac{\partial w}{\partial t}-P\frac{\partial^2 w}{\partial x^2}+EI\frac{\partial^4 w}{\partial x^4}+\rho_f A_f\frac{dV}{dt}\frac{\partial w}{\partial x}-\frac{EA_p}{2L}\frac{\partial^2 w}{\partial x^2}\int_0^L\left(\frac{\partial w}{\partial x}\right)^2 dx+f\left(x_0,t\right)\delta\left(x-x_0\right)=0\end{aligned}\tag{22}$$

Where $f\left(x_0,t\right)$ represents the external force generated by the controller, defined as

$$f\left(x_0,t\right)=k_{NES}\left(y-w\right)^3+c_{NES}\left(\frac{dy}{dt}-\frac{dw}{dt}\right)\tag{23}$$

By substituting (23) in (22), we obtain the following equation

$$\begin{aligned}&\left(\rho_p A_p+\rho_f A_f\right)\frac{\partial^2 w}{\partial t^2}+2\rho_f A_f\left(V_0+V_1\sin(\Omega t)\right)\frac{\partial^2 w}{\partial x\partial t}+\rho_f A_f\left(V_0+V_1\sin(\Omega t)\right)^2\frac{\partial^2 w}{\partial x^2}\\&+\rho_f A_f\frac{dV}{dt}\frac{\partial w}{\partial x}-\frac{EA_p}{2L}\frac{\partial^2 w}{\partial x^2}\int_0^L\left(\frac{\partial w}{\partial x}\right)^2 dx+\left(k_{NES}\left(y-w\right)^3+c_{NES}\left(\frac{dy}{dt}-\frac{dw}{dt}\right)\right)\delta\left(x-x_0\right)\\&+c\frac{\partial w}{\partial t}-P\frac{\partial^2 w}{\partial x^2}+EI\frac{\partial^4 w}{\partial x^4}=0\end{aligned}\tag{24}$$

According to (Zhao et *al*. 2018b) and fig. 7, the equation of motion of the controller is expressed as:

$$m_{NES}\frac{d^2 y}{dt^2}+k_{NES}\left(y-w\right)^3+c_{NES}\left(\frac{dy}{dt}-\frac{dw}{dt}\right)=0\tag{25}$$

Hence pipeline conveying fluid with time dependent velocity with integrated vibration controller is governed by the following system of coupled equations:

$$\left\{\begin{aligned}&\left(\rho_p A_p+\rho_f A_f\right)\frac{\partial^2 w}{\partial t^2}+2\rho_f A_f\left(V_0+V_1\sin(\Omega t)\right)\frac{\partial^2 w}{\partial x\partial t}+\rho_f A_f\left(V_0+V_1\sin(\Omega t)\right)^2\frac{\partial^2 w}{\partial x^2}\\&+c\frac{\partial w}{\partial t}-P\frac{\partial^2 w}{\partial x^2}+EI\frac{\partial^4 w}{\partial x^4}+\rho_f A_f\frac{dV}{dt}\frac{\partial w}{\partial x}-\frac{EA_p}{2L}\frac{\partial^2 w}{\partial x^2}\int_0^L\left(\frac{\partial w}{\partial x}\right)^2 dx\\&+\left(k_{NES}\left(y-w\right)^3+c_{NES}\left(\frac{dy}{dt}-\frac{dw}{dt}\right)\right)\delta\left(x-x_0\right)=0\\&m_{NES}\frac{d^2 y}{dt^2}+k_{NES}\left(y-w\right)^3+c_{NES}\left(\frac{dy}{dt}-\frac{dw}{dt}\right)=0\end{aligned}\right.\tag{26}$$

The following dimensionless variables are introduced:

$$\begin{aligned}&x=L\xi;\ w=L\eta;\ \tau=\omega_0 t;\ \omega_0=\frac{1}{L^2}\sqrt{\frac{EI}{M}};\ \Psi=\frac{\Omega}{\omega_0};\ \mu=\frac{cL^2}{\sqrt{EIM}};\ \beta=\frac{\rho_f A_f}{\rho_p A_p+\rho_f A_f}\\&\vartheta_0=V_0 L\sqrt{\frac{\rho_f A_f}{EI}};\ \vartheta_1=V_1 L\sqrt{\frac{\rho_f A_f}{EI}};\ \gamma=\frac{PL^2}{EI};\ \kappa=\frac{A_p L^2}{2I};\ M=\rho_p A_p+\rho_f A_f\\&\varepsilon_1=\frac{m_{NES}}{M}\prec\prec 1;\ K_{NES}=\frac{k_{NES}L^2}{EI};\ C_{NES}=\frac{c_{NES}L^4}{\sqrt{EIM}};\ \lambda_1=\frac{k_{NES}}{EI};\ \lambda_2=\frac{c_{NES}}{\sqrt{EIM}}\end{aligned}\tag{27}$$

Substituting these variables into the governing equations and performing the corresponding mathematical manipulations lead to the following dimensionless system:

$$\frac{\partial^2\eta}{\partial\tau^2}+\frac{\partial^4\eta}{\partial\xi^4}+\mu\frac{\partial\eta}{\partial\tau}+2\sqrt{\beta}\vartheta_0\frac{\partial^2\eta}{\partial\tau\partial\xi}+\left(\vartheta_0^2-\gamma\right)\frac{\partial^2\eta}{\partial\xi^2}-\kappa\frac{\partial^2\eta}{\partial\xi^2}\int_0^1\left(\frac{\partial\eta}{\partial\xi}\right)^2d\xi+2\sqrt{\beta}\vartheta_1\sin\left(\Psi\tau\right)\frac{\partial^2\eta}{\partial\tau\partial\xi}$$
$$+2\vartheta_0\vartheta_1\sin\left(\Psi\tau\right)\frac{\partial^2\eta}{\partial\xi^2}+\sqrt{\beta}\vartheta_1\Psi\cos\left(\Psi\tau\right)\frac{\partial\eta}{\partial\xi}+\left[\lambda_1\left(\bar{\eta}-\eta\right)^3+\lambda_2\left(\frac{d\bar{\eta}}{d\tau}-\frac{d\eta}{d\tau}\right)\right]\delta\left(\xi-\xi_0\right)=0 \tag{28a}$$

$$\varepsilon_1\frac{d^2\bar{\eta}}{d\tau^2}+K_{NES}\left(\bar{\eta}-\eta\right)^3+C_{NES}\left(\frac{d\bar{\eta}}{d\tau}-\frac{d\eta}{d\tau}\right)=0 \tag{28b}$$

To derive the modal equations, the Galerkin method is employed. The transverse displacement is approximated by the following modal expansion:

$$\eta\left(\xi,\tau\right)=\sum_{n=1}^{\infty}q_n\left(\tau\right)\sin\left(n\pi\xi\right) \tag{29}$$

here $q_n\left(\tau\right)$ denotes the generalized coordinate associated with the nth vibration mode and $\varphi_n\left(\xi\right)=\sin\left(n\pi\xi\right)$ is the corresponding mode shape satisfying the boundary conditions.

Following Dai et al. (2015b) and Wang, Hu, and Zhong (2013b), the Galerkin expansion is truncated to the fundamental vibration mode ($n = 1$), since this mode is expected to contain most of the vibration energy and therefore provides an accurate first approximation of the system dynamics.

Substituting the assumed modal expansion into the governing equations finally yields

$$\ddot{q}+\mu\dot{q}+\left(\varpi^2-\varsigma\sin\left(\Psi\tau\right)\right)q+\beta_1q^3+\lambda_1\left(\bar{\eta}-q\right)^3+\lambda_2\left(\dot{\bar{\eta}}-\dot{q}\right)=0 \tag{30a}$$

$$\varepsilon_1\ddot{\bar{\eta}}+K_{NES}\left(\bar{\eta}-q\right)^3+C_{NES}\left(\dot{\bar{\eta}}-\dot{q}\right)=0 \tag{30b}$$

5.1. Effects of the Vibration Controller on the Time Response Of The Pipeline

The time responses of the controlled pipeline are obtained by numerically integrating the governing equations using the fourth-order Runge–Kutta method. The resulting displacement histories are presented in Figures 8 and 9.

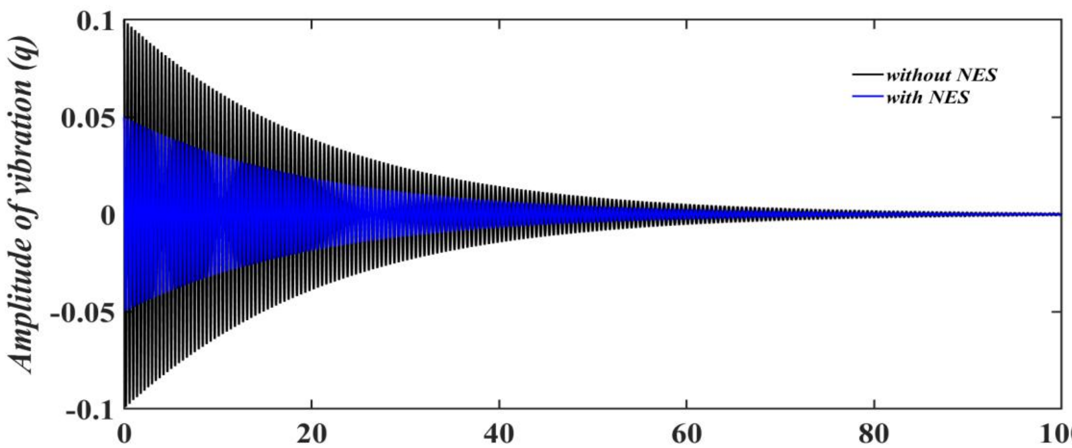

Figure 8: Influence of the vibration controller on the time displacement response of the fluid conveying pipeline, for $\vartheta_0 = 0.0057$, Ω=13.60 and $\xi_0 = \dfrac{1}{2}$.

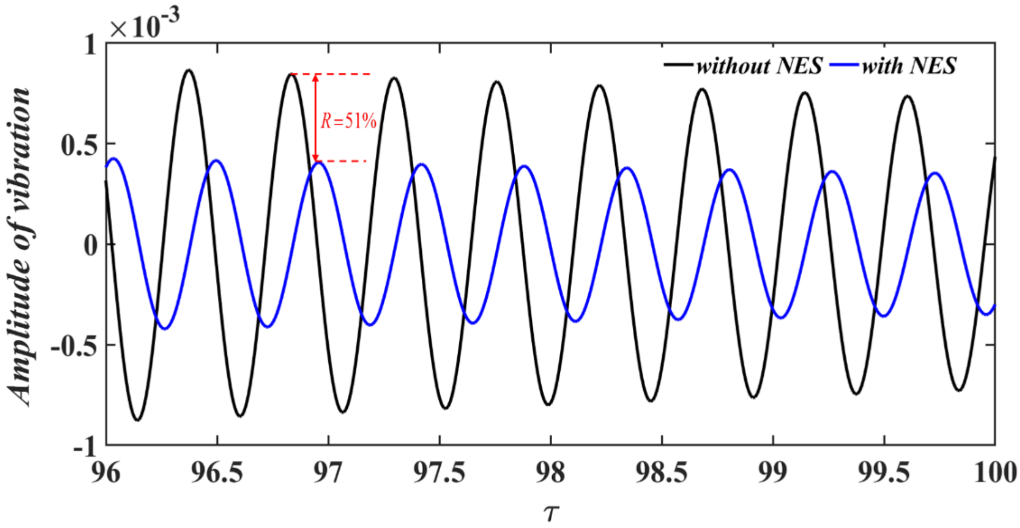

Figure 9: Vibration attenuation percentage achieved by the vibration controller.

Figure 8 compares the transverse displacement responses of the pipeline with and without the integrated vibration controller. The results clearly show that the presence of the controller significantly reduces the vibration amplitude. This attenuation is mainly attributed to the viscoelastic properties and the inertial effect of the nonlinear energy sink, which efficiently dissipates part of the vibration energy. Consequently, the controller enhances the dynamic stability of the pipeline and is expected to contribute to extending its service life.

Figure 9 presents the vibration attenuation percentage obtained with the proposed controller. A maximum reduction of 51% is achieved $\varepsilon_1 = 0.0001$, $K_{nes} = 1$ and $C_{nes} = 0.1$, demonstrating the effectiveness of the proposed vibration control strategy. Nevertheless, a comprehensive stability analysis is still required to determine the optimal controller parameters ensuring both maximum vibration attenuation and robust dynamic performance. This aspect will be addressed in future work.

6. Conclusion and Perspectives

This study investigated the nonlinear dynamic behaviour of a pipeline conveying a fluid with time-dependent velocity, considering both the uncontrolled configuration and the configuration equipped with a vibration controller. First, the influence of the dimensionless mean flow velocity on the natural frequencies of the pipeline was analysed. The results showed that increasing the mean flow velocity leads to divergence of the first and second vibration modes, with critical dimensionless flow velocities of 4.33 and 6.95, respectively.
The influence of the critical mean flow velocity on the transient displacement response of the pipeline was subsequently examined. The results demonstrated that the pipeline oscillates about a stable equilibrium position when the mean flow velocity remains below the critical value, whereas operation at the critical velocity results in oscillations about an unstable equilibrium position, thereby compromising the dynamic stability of the structure.
Finally, the effectiveness of a Nonlinear Energy Sink (NES) was evaluated as a passive vibration control device. The proposed controller achieved a vibration attenuation of 51%, demonstrating its ability to significantly reduce the vibration amplitude and improve the dynamic performance of the pipeline.
Future work will focus on the stability analysis of the controlled system in order to determine the optimal controller parameters for maximum vibration attenuation. In addition, the development of an experimental prototype incorporating the thermal effects of the conveyed fluid will provide further validation of the theoretical predictions presented in this study.

Financial supports

No funds, grants or other financial support was received to conduct this study or to prepare the manuscript.

Competing interests

The authors declare that they have no known competing financial interests or personal relationships that could have appeared to influence the work reported in this paper.

References

Cao, Y., Yan, G., Lu, J., Qi, W., Zhao, T., Yu, D., Cai, L., Li, Y., & Zhang, W. (2025). Vibration mitigation and dynamics of pipeline system with nonlinear soft clamp by a nonlinear energy sink. *International Journal of Non-Linear Mechanics, 170*, 104990. https://doi.org/10.1016/j.ijnonlinmec.2024.104990

Dai, H. L., Wang, L., Abdelkefi, A., & Ni, Q. (2015a). On nonlinear behavior and buckling of fluid-transporting nanotubes. *International Journal of Engineering Science, 87*, 13–22. https://doi.org/10.1016/j.ijengsci.2014.11.005

Gao, P., Yu, T., Zhang, Y., Wang, J., & Zhai, J. (2021). Vibration analysis and control technologies of hydraulic pipeline system in aircraft: A review. *Chinese Journal of Aeronautics, 34*(4), 83–114.

Hao, M. Y., Ding, H., Mao, X. Y., & Chen, L. Q. (2023a). Stability and nonlinear response analysis of parametric vibration for elastically constrained pipes conveying pulsating fluid. *Acta Mechanica Solida Sinica, 36*(2), 230–240. https://doi.org/10.1007/s10338-022-00370-z

Hao, M. Y., Ding, H., Mao, X. Y., & Chen, L. Q. (2023b). Stability and nonlinear response analysis of parametric vibration for elastically constrained pipes conveying pulsating fluid. *Acta Mechanica Solida Sinica, 36*(2), 230–240. https://doi.org/10.1007/s10338-022-00370-z

Karrech, A., Abdolahpour, M., An, H., Bransby, F., Draper, S., Hou, Z., & Watson, P. (2024). Non-linear vibration of free spanning subsea pipelines with multi-dimensional mid-plane stretching. *Engineering Structures, 301*, 117265. https://doi.org/10.1016/j.engstruct.2023.117265

Kesimli, A., Bağdatlı, S. M., & Çanakcı, S. (2016). Free vibrations of fluid conveying pipe with intermediate support. *Research on Engineering Structures and Materials*. https://doi.org/10.17515/resm2015.18me0825

Luo, Y., & Zhang, D. (2022). Dynamic analysis of an axially moving underwater pipe conveying pulsating fluid. *Frontiers in Marine Science, 9*. https://doi.org/10.3389/fmars.2022.982374

Mamaghani, A. E., Khadem, S. E., & Bab, S. (2016). Vibration control of a pipe conveying fluid under external periodic excitation using a nonlinear energy sink. *Nonlinear Dynamics, 86*(3), 1761–1795. https://doi.org/10.1007/s11071-016-2992-x

Mao, X. Y., Ding, H., & Chen, L. Q. (2016). Steady-state response of a fluid-conveying pipe with 3:1 internal resonance in supercritical regime. *Nonlinear Dynamics, 86*(2), 795–809. https://doi.org/10.1007/s11071-016-2924-9

Panda, L. N., & Kar, R. C. (2007). Nonlinear dynamics of a pipe conveying pulsating fluid with parametric and internal resonances. *Nonlinear Dynamics, 49*(1–2), 9–30. https://doi.org/10.1007/s11071-006-9100-6

Tan, X., & Ding, H. (2020). Parametric resonances of Timoshenko pipes conveying pulsating high-speed fluids. *Journal of Sound and Vibration, 485*, 115594. https://doi.org/10.1016/j.jsv.2020.115594

Tang, Y., Wang, G., & Ding, Q. (2022a). Nonlinear fractional-order dynamic stability of fluid-conveying pipes constituted by viscoelastic materials with time-dependent velocity. *Acta Mechanica Solida Sinica, 35*(5), 733–745. https://doi.org/10.1007/s10338-022-00328-1

Tang, Y., Wang, G., & Ding, Q. (2022b). Nonlinear fractional-order dynamic stability of fluid-conveying pipes constituted by viscoelastic materials with time-dependent velocity. *Acta Mechanica Solida Sinica, 35*(5), 733–745. https://doi.org/10.1007/s10338-022-00328-1

Tang, Y., Zhen, Y., & Fang, B. (2018). Nonlinear vibration analysis of a fractional dynamic model for the viscoelastic pipe conveying fluid. *Applied Mathematical Modelling, 56*, 123–136. https://doi.org/10.1016/j.apm.2017.11.022

Wang, L., Hu, Z., & Zhong, Z. (2013a). Non-linear dynamical analysis for an axially moving beam with finite deformation. *International Journal of Non-Linear Mechanics, 54*, 5–21. https://doi.org/10.1016/j.ijnonlinmec.2013.03.004

Wang, Y., Luo, S., Yang, M., Qin, T., Zhao, J., & Yu, G. (2022). Analysis of marine risers subjected to shoal/deep water in the installation process. *Polish Maritime Research, 29*(2), 43–54. https://doi.org/10.2478/pomr-2022-0016

Wei, S., Yan, X., Li, X., Ding, H., & Chen, L. Q. (2023a). Parametric vibration of a nonlinearly supported pipe conveying pulsating fluid. *Nonlinear Dynamics, 111*(18), 16643–16661. https://doi.org/10.1007/s11071-023-08761-8

Yang, T. Z., Yang, X. D., Li, Y., & Fang, B. (2014). Passive and adaptive vibration suppression of pipes conveying fluid with variable velocity. *Journal of Vibration and Control, 20*(9), 1293–1300. https://doi.org/10.1177/1077546313480547

Yang, T., Liu, T., Tang, Y., Hou, S., & Lv, X. (2019). Enhanced targeted energy transfer for adaptive vibration suppression of pipes conveying fluid. *Nonlinear Dynamics, 97*(3), 1937–1944. https://doi.org/10.1007/s11071-018-4581-7

Zhang, W., Chang, Z. Y., & Chen, J. (2023). Vibration reduction for an asymmetric elastically supported beam coupled to an inertial nonlinear energy sink. *Journal of Vibration Engineering and Technologies, 11*(4), 1711–1723. https://doi.org/10.1007/s42417-022-00666-x

Zhao, X. Y., Zhang, Y. W., Ding, H., & Chen, L. Q. (2018a). Vibration suppression of a nonlinear fluid-conveying pipe under harmonic foundation displacement excitation via nonlinear energy sink. *International Journal of Applied Mechanics, 10*(9). https://doi.org/10.1142/S1758825118500965

Zhao, X. Y., Zhang, Y. W., Ding, H., & Chen, L. Q. (2018b). Vibration suppression of a nonlinear fluid-conveying pipe under harmonic foundation displacement excitation via nonlinear energy sink. *International Journal of Applied Mechanics, 10*(9). https://doi.org/10.1142/S1758825118500965

Zhou, K., Yi, H. R., Dai, H. L., Yan, H., Guo, Z. L., Xiong, F. R., Ni, Q., Hagedorn, P., & Wang, L. (2022). Nonlinear analysis of L-shaped pipe conveying fluid with the aid of absolute nodal coordinate formulation. *Nonlinear Dynamics* ***107****, 391-412.* https://doi.org/10.1007/s11071-021-07016-8